Czech Society for Nondestructive Testing
32nd European Conference on Acoustic Emission Testing
Prague, Czech Republic, September 07-09, 2016

MEASUREMENT OF ELECTROMAGNETIC EMISSION AS A TOOL TO STUDY FRACTURE PROCESSES OF CARBON FIBRE REINFORCED POLYMERS

Sebastian O. GADE, Philipp POTSTADA, Benjamin B ALACA, Markus G. R. SAUSE

Experimental Physics II, University of Augsburg; Augsburg, Germany
Phone: +49 821 598 3407; e-mail: sebastian.gade@physik.uni-augsburg.de

Abstract
In addition to acoustic emission (AE), fracture of solid materials is often accompanied by electromagnetic emission (EME). These electromagnetic fields arise due to the separation, displacement or movement of charges and their temporal characteristics and spatial distributions are closely connected to the dynamics of the fracture processes and the material's physical properties. The measurement of EME provides a method to directly access information of microscopic failure, such as crack velocity, crack duration, crack wall vibration frequencies or crack orientation. The use of capacitive sensors to detect EME offers a linear transfer function for the frequency range of interest. Measurements of EME and AE were performed during interlaminar crack growth of unidirectional carbon fibre reinforced polymers (CFRP) under mode I and mode II load as well as during fracture of cross-plied CFRP specimens under flexural and tensile loading. Different EME signals are observed and attempts are being made to attribute certain EME signal characteristics to specific fracture processes.

Keywords: electromagnetic emission, acoustic emission, fibre reinforced polymers, fracture mechanics

1. Introduction

Carbon fibre reinforced polymers (CFRP) offer a variety of unique physical properties which make these materials favourable for various applications. Especially their mechanical properties make these materials attractive for engineering purposes. Besides their wide range of application, e.g. in aerospace industry, CFRP materials are still subject of research. Due to their complex microstructure and anisotropic properties their failure behaviour is complicated and their ultimate limits are hard to predict. One possible method to study the fracture processes is the acquisition and analysis of signals generated during these processes. These signals can be acoustic emission (AE) signals, measured as transient displacements at the surface of the material, and electromagnetic emission (EME) signals, measured in the vicinity of the fracture. Both types of signals contain information about their sources, i.e. the fracture processes. The study of AE generated by fracture is a well-established method but is nevertheless still subject to current research. On the other hand, the study of EME generated by fracture of composites, though there has been some research in the past [1-3], has not been progressed this far. EME has been reported for various materials and failure modes [2,4-7] and numerous theories for the origin of these electromagnetic fields were proposed [8-10]. The source mechanisms may well be completely different for different materials and failure modes, but on a fundamental basis electromagnetic fields are generated by charges and their dynamics.

Electromagnetic emission, as referred to in this text, is described in terms of electric fields in the frequency range of kHz to MHz, since these are directly measured as voltage signals by our capacitive sensors [11].

The different components of CFRP and their fracture processes are likely to generate different kinds of EME signals (in fact, different EME signal characteristics for the individual components have already been reported [1,12]). Furthermore, in contrast to the emitted

acoustic signals, the EME signals can be measured almost undisturbed, i.e. are not influenced by the specimen's material and geometry. This advantage of EME over AE may prove to be particularly beneficial in highly anisotropic composite materials.
In the context of a recent research project, we studied EME generation of CFRP materials and its components. In this study we present EME signals generated by interlaminar crack growth of unidirectional CFRP under mode I and mode II load as well as EME signals generated by fracture of cross-ply CFRP specimens under flexural and tensile loading. A discussion of the acquired EME signals is made with respect to the differences when comparing signals generated by different fracture processes and when comparing the EME signals to the accompanying AE signals.

2. Experimental set-up and results

2.1 Testing and acquisition set-ups

In order to detect EME signals generated by different failure modes in CFRP a variety of different testing procedures were conducted to induce CFRP fracture under various loading conditions. CFRP specimens of different ply stacking sequences were fabricated from unidirectional Sigrafil CE1250-230-39 carbon/epoxy prepreg laminate.
Most of the applied test fixtures, with the exception of the tensile test fixture presented in section 2.2.4, were manufactured from non-conductive materials to reduce interfering influences of conductive materials on the EME acquisition. PMMA was used for most parts while supports were made from PVC and bolts were made from POM. The mechanical load is introduced using a tube of pultruded glass-fibre reinforced plastic (GFRP).
Two different types of acoustic emission sensors were used, a KRBBN-PC point contact sensor and a multi resonant, "wideband differential" (WD) sensor (Physical Acoustics). The point contact sensor offers an almost linear transfer function and a greater band width but suffers from a weaker sensitivity when compared to the WD sensor. For the DCB and ENF tests measurable EME signals could only be detected for macroscopic crack propagation. Thus, the KRBBN-PC sensor was chosen to measure the accompanying, high amplitude acoustic emission signals. During fracture of CFRP specimens during flexure and tensile testing EME signals with a wide range of amplitudes could be measured. Therefore, in order to measure the accompanying AE signals, the more sensitive WD sensor was chosen. For both AE sensor types the AE signals were amplified by a 2/4/6 pre-amplifier without use of an internal bandpass filter. For distinguishability AE signals recorded with the KRBBN-PC sensor are plotted in blue throughout this text while AE signals recorded with the WD sensor are plotted in pink.
For the EME signal detection two amplification stages were used. The first preamplifier, which is located inside the shielding enclosure, is a junction field effect transistor (n-channel JFET 2SK932-22) in a common source circuit with a 10 MΩ input resistor, with a total amplification of 20 dB. This preamplifier is directly connected to the wire forming the capacitive sensor. The voltage signal then is further amplified by a commercially available low frequency amplifier (UBBV-NF35, Aaronia AG). The total gain was adjustable with a potential divider between the two amplifiers. A PCI-2 acquisition card (Mistras corporation, software: AEwin) was used to record the signals. For flexural an tensile testing, AE and EME signals were acquired in synchronized mode, while for mode I and mode II testing, AE and EME signals were triggered independently following the settings of Table 1.
Since the field distributions of the EME generated by fracture have been shown to exhibit pronounced directional characteristics [7,9,13] the positions of the EME sensors were chosen accordingly.

All set-ups were electrically shielded by a grounded metallic shielding enclosure. A detailed description of this acquisition circuit and the shielding measures can be found in [12]. Table 1 summarizes all acquisition parameters used.

Table. 1. Parameters used for EME and AE acquisition

Set-up		DCB	ENF	Flexural	Tensile
Amplif. AE	[dB]	20	20	40	40
Amplif. EME	[dB]	40	40	40	46
Threshold AE	[dB_{AE}]	40	40	30	35
Threshold EME	[dB_{AE}]	28	27	35	38
Sample rate AE	[MS/s]	10	10	10	10
Sample rate EME	[MS/s]	5	2	10	10
Band pass*	[kHz]	1-3000	1-3000	1-3000	1-3000
PDT AE	[µs]	10	10	synchronized	synchronized
HDT AE	[µs]	80	80	synchronized	synchronized
HLT AE	[µs]	300	300	300	300
PDT EME	[µs]	20	20	synchronized	synchronized
HDT EME	[µs]	1200	1200	synchronized	synchronized
HLT EME	[µs]	200	200	300	300
(* band pass of acquisition board, AE sensors exhibit smaller band widths)					

2.2. Mode I - DCB test

2.2.1 Set-up

Figure 1 shows the DCB test set-up which was manufactured to conform with the requirements of ASTM D5528. CFRP specimens with a $[0_7]_{sym}$ ply stacking sequence and dimensions of 155 mm x 25 mm x 3 mm were used. As crack initiation side an ETFE insert of 60 mm length was embedded at the centre of the laminate plies. PMMA loading blocks were added using an adhesive. For the detection of the acoustic emission signals, a point contact sensor is mounted on top of the specimen. A copper wire attached to the upper face of the specimen is used as EME sensor.

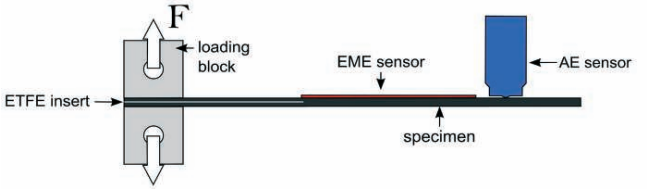

Fig. 1. Schematic of DCB test set-up.

The load was applied displacement controlled by an universal testing machine (Zwick ZT 5.0) with a constant cross head velocity of 2 mm/min and is measured by a 5 kN Xforce HP load cell. The tests were conducted in two stages. The first stage was carried out to induce a precrack to the specimen, starting from the ETFE insert. In the second stage the precrack then serves as a natural crack starter, when the crack slowly propagates along the midplane of the specimen.

2.2.2 Results

Figure 2 shows exemplary EME and AE signals generated during the first testing stage, i.e. during the initiation and propagation of the first crack starting at the ETFE insert. The obtained AE and EME signals show some variation in amplitude and characteristic which is attributed to variations in crack length and crack propagation. The EME signals all start with a fast rise in amplitude which then slowly decreases, superimposed by oscillations. The rise is attributed to the crack propagation where charges are separated while the characteristic decrease results from the 1kHz high pass filter of the used acquisition board. The oscillations are attributed to vibrations of the electrified crack surfaces and the dynamics of the specimen and EME sensor during and after crack propagation.
Applying a 4kHz high pass filter (6th order Butterworth) removes most of the low frequency signal components attributed to the charges resulting from crack extension, leaving only the oscillations attributed to crack wall vibration and specimen movement (see figure 2). A comparison to the corresponding AE signals reveals some similarities between EME and AE signals like similar rise times, frequencies and signal duration.

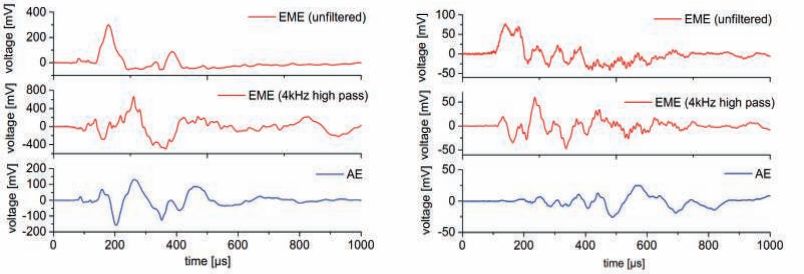

Fig. 2. AE and EME signals recorded during precracking stage of DCB testing.

In the second stage, starting at the precrack, the crack slowly begins to propagate within the specimen. During this phase various EME signals could be measured. Three basic EME signal characteristics were observed. The first kind of EME signal consists of a very fast rise and a slow decay representing the high pass filter of the acquisition board. This signal shape is the response function of our acquisition set-up to a step-function as input voltage. Figure 3 (left) shows an exemplary EME signal that consists of several signals of this type occurring in rapid succession. EME signals with these characteristics are also observed during fracture of carbon fibres [1,12] where the fast signal rise is attributed to the very short crack length (<10 µm) and therefore very short crack propagation times (order of nanoseconds [14]). The point contact AE sensor (with 20dB amplification) did not detect any AE signals that correlate to this type of EME signals. Only by the more sensitive WD AE sensor with 40 dB amplification corresponding AE signals were detected (see figure 3, left).

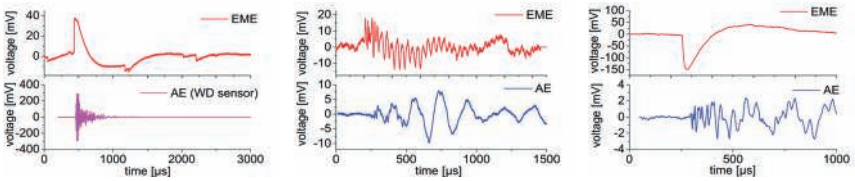

Fig. 3. AE and EME signals recorded during crack propagation stage of DCB testing.

A second type of EME signal is shown in figure 3 (middle). It resembles the precrack signals with superimposed oscillations, but exhibits smaller amplitudes for both, EME and AE signals.
Figure 3 (right) shows a third kind of observed EME signal which exhibits a slower rise than signal type one. No superimposed oscillations are measured with this type of signal. For the remaining EME signals the shape could be considered as combinations of these three base types.

2.3 Mode II - ENF tests

2.3.1 Set-up

The ENF test set-up was manufactured according to ASTM D7905. A schematic of the set-up is shown in figure 4. CFRP specimens with a $[0_8]_{sym}$ ply stacking sequence and dimensions of 180 mm x 25 mm x 3.5 mm were used. As crack initiation side, an ETFE insert of 45 mm length was embedded at one side of the specimens. A point contact sensor was placed at the surface of the specimens to detect the AE signals. A pair of copper wires is placed near the crack tip, consisting of a "detecting" wire (attached to the acquisition chain) and a grounded wire, thus forming a capacitor type EME sensor.

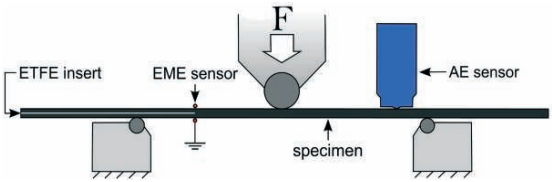

Fig. 4. Schematic of ENF test set-up.

As for the DCB tests, the ENF tests are carried out in two stages, with the load applied displacement controlled with a cross head velocity of 2 mm/min. The first stage only induces a precrack while in the second stage the crack propagation occurs. Here, between the two stages, the specimen position is adjusted to account for the new crack tip position and to match with the position of the EME sensor.

2.3.2 Results

The EME signals recorded during the precracking stages of the DCB and ENF tests are comparable in terms of signal characteristics and rise times. As for the mode I tests, the first rise of the EME signals are considered to contain information about the crack propagation. When the crack stops its propagation, no new charges are generated and the signal amplitude starts to decrease. Superimposed oscillations are attributed to microscopic and macroscopic movement of the charged crack surfaces. Exemplary EME signals are shown in figure 5.

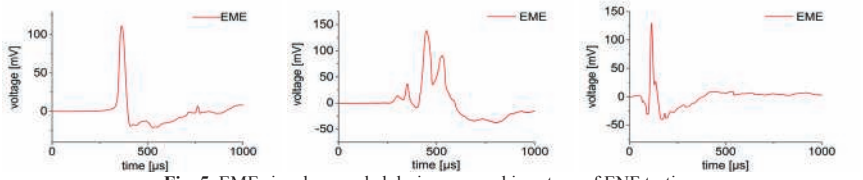

Fig. 5. EME signals recorded during precracking stage of ENF testing.

In contrast to the DCB tests, the crack propagation in the second stage is not entirely stable. Here, starting at the precrack, the crack initially propagates slowly before unstable crack

propagation occurs. This unstable crack growth generates strong EME signals which are comparable to the ones recorded during the first, precracking stage. Figure 6 (left) exemplarily shows an EME signal of this kind. Another kind, which was also observed during the DCB tests, is shown in figure 6 (middle). Signals recorded after this unstable crack propagation are considered to be generated by secondary processes since the macroscopic crack tip already is out of the detection range of the EME sensor. An example of such EME signals is shown in figure 6 (right). The kind of EME signal with the step-function like rise in amplitude was not observed during the ENF tests.
In contrast to the distinct and repeatable EME signal types seen in testing of polymers [13] or carbon fibres [12] the EME signals of composite failure tend to cover a broad spectrum of different signatures reflecting the complexity of the fracture process seen in composite materials.

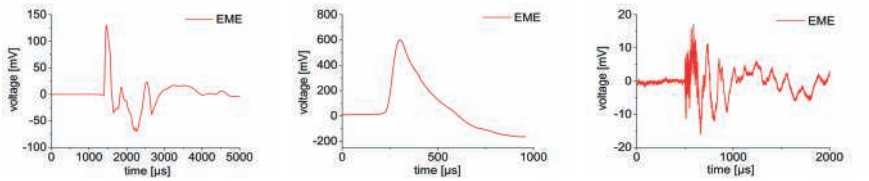

Fig. 6. EME signals recorded during crack propagation stage of ENF testing.

2.4 Flexure test

2.4.1 Set-up

On the basis of DIN EN ISO 14125 a three point bending test set-up was manufactured to induce fracture of cross-ply CFRP specimens. These tests were conducted on specimens with different ply stacking sequences to obtain a variety of failure modes and crack surface orientations. Stacking sequences of $[0_2,90_3]_{sym}$, $[0,90_2,0,90]_{sym}$ and $[0_2,90,0,90]_{sym}$ were chosen. The specimens' dimensions are 95 mm x 15 mm x 2.2 mm. The acoustic emission signals were detected at the specimen surface by an attached WD sensor. A pair of copper wires, placed near the region of the load nose, serves as EME sensor. The load was applied displacement controlled, with a cross head velocity of 1mm/min.

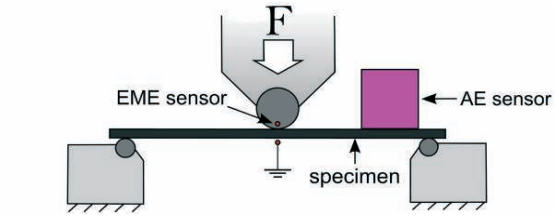

Fig. 7. Schematic of flexure test set-up.

2.4.2 Results

The fracture of the CFRP specimens during the flexure test progresses in multiple steps. Initial failure occurs in the upmost layer of the specimens directly beneath the load nose. Here, compressive failure of the 0°-layer occurs. During this first phase of specimen failure multiple EME signals could be measured. Figure 8 (left) shows an exemplary EME and AE signal pair of this initial failure.

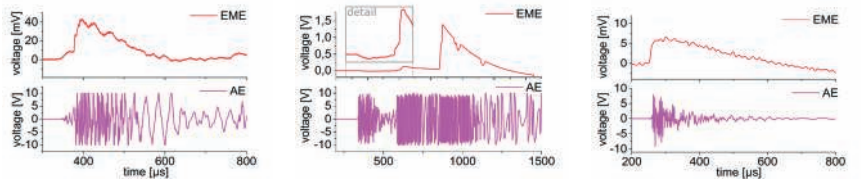

Fig. 8. AE and EME signals recorded during flexure tests. Left: Signals from initial failure of first layer. Middle and right: Signals from final failure (Middle: signal exceeding detection range of amplifier results in signal saturation).

Figures 8 (middle and right) show AE and EME signals recorded during the final failure of the specimens. The stronger signals (figure 8, middle) may be attributed to the occurrence of larger cracks, e.g. inter-ply delamination. Other signals, as exemplarily shown in figure 8 (right), exhibit smaller amplitudes for both, AE and EME, signals and therefore are attributed to weaker source mechanisms.

All measured EME signals recorded during the flexure tests exhibit a similar characteristic shape. An initial rise in amplitude is followed by a slower decrease. The time constant of the decrease is caused by the 1 kHz high pass filter of our acquisition board. However, the rise times are assumed to correlate with crack propagation times, which are measured in the order of 10^{-6} s to 10^{-4} s.

2.5 Tensile tests

2.5.1 Set-up

The tensile tests were conducted in accordance with DIN EN ISO 527-4. The tests were performed in a universal testing machine Zwick 250 with hydraulic grips. The load is applied displacement controlled with a velocity of 1 mm/min. Here, a test fixture made from non-conductive materials was not feasible to apply. To eliminate influences of the testing machine and the metallic components of the test fixture on the detected EME signals, a small shielding enclosure was chosen instead, to only contain parts of the specimen, the AE and EME sensors and one EME pre-amplifier.

CFRP specimens with a $[0,90,0,90]_{sym}$ stacking sequence were used. At both ends the specimens were reinforced with end tabs made of cross ply laminates. The specimens dimensions were 178mm x 15 mm. The specimen thickness was 1 mm at the centre and 4 mm at the reinforced ends. To ensure the induced failure to occur at the specimen centre (where the EME sensor is located) additional notches of 2.5 mm length were added (see figure 9).

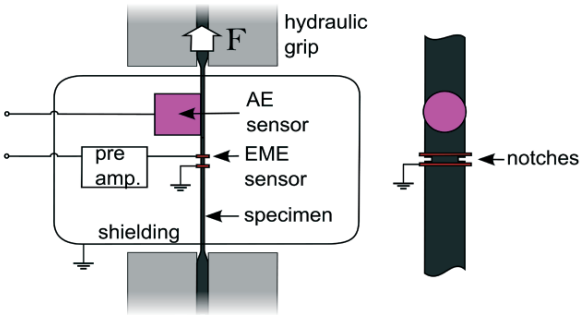

Fig. 9. Schematic of tensile test set-up. Left: side view of set-up, with shielding enclosure. Right: front view of specimen.

For the AE detection a WD sensor was attached to the specimen surface. Two loops of copper wire, forming a kind of capacitor, were placed around the specimens near the centre of the specimen as depicted in figure 9.

2.5.2 Results

Although the partially conducting CFRP specimens penetrate the shielding enclosure and therefore weaken its shielding effectiveness [12], numerous EME signals could be detected during the fracture tests. Due to the chosen cross-ply stacking sequence different failure modes occur during testing, i.e. fibre fracture, matrix fracture and various types of interfacial failure. Microscopic failure arises long before the final failure of the specimens. Figure 10 shows AE and EME signals generated during the early stage of loading.

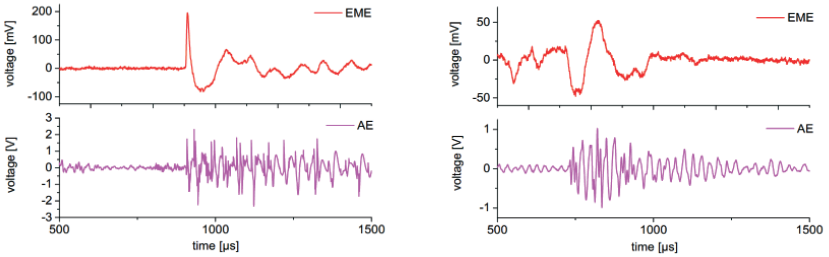

Fig. 10. AE and EME signals recorded before final failure of specimens during tensile tests.

When final failure of the specimens occurs, numerous AE and EME signal pairs were detected. These signals exhibit high amplitudes which most of the times exceed the maximum input voltage of the acquisition equipment which results in saturated signals. Figure 11 shows exemplary AE and EME signals recorded during this final failure. As seen from the voltage scale the EME signals are also extraordinary strong, therefore indicating a general relationship between the occurrence of macroscopic damage and strong EME release.

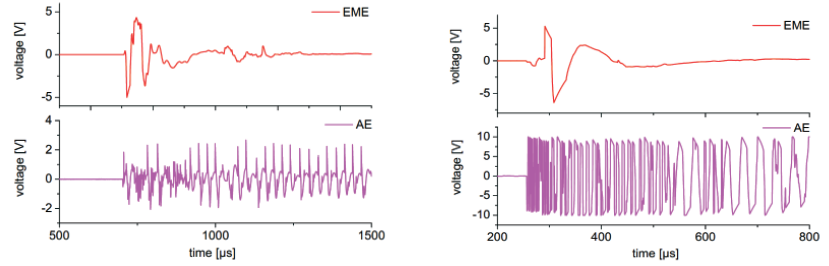

Fig. 11. AE and EME signals recorded during final failure of specimens during tensile tests (partially clipped).

3. Summary and Conclusion

EME signals could be detected for all tests. Nevertheless, the total amount of detected EME signals was small when compared to the amount of detected AE signals. This discrepancy is mainly attributed to the weaker sensitivity of the EME acquisition set-up which depends on various factors but is in particular limited by the considerable dependence of the EME signal strength on source-sensor-distance.

Both methods, AE and EME, are able to detect the formation of microscopic damage in fibre reinforced composites. For EME the similarity in the band width is attributed to the vibrations of newly generated crack surfaces, which also forms the source for acoustic emission.

The EME signal components not accessible to AE may offer further applications. Most EME theories assume some kind of electrification of the new crack surfaces, e.g. via charge separation. The build-up of this charge distribution continues as long as the crack propagates. Therefore, the EME signal rise times are assumed to correlate with crack propagation times, which should allow for the derivation of the crack tip position as function of time. For known maximum crack extensions this even allows for the derivation of the time dependent crack propagation velocities.

For the acoustic emission signals, the analysis of its frequency components, e.g. by applying pattern recognition techniques, to identify the source mechanisms of the signals in composite materials is a well-established method. Similar techniques should also be applicable to EME signals but will require a higher signal yield. In this regard, a combined approach of AE and EME analysis seems to be the most promising.

The evaluation of the amplitudes of EME signals proves to be more difficult since the detected EME amplitude not only depends on the source strength but also substantially depends on source-sensor-distance as well as source-sensor orientation.

The applied acquisition set-up also demonstrates the close similarity of information of the AE and EME signals. However, EME acquisition set-ups using capacitive sensors can easily be built to exhibit almost perfectly flat transfer functions. Herein lies a huge advantage of the EME detection, as acoustic wave propagation is shaped by the propagation medium and propagation path.

Acknowledgements

This research is funded by the DFG as part of the project ”Relation of electromagnetic and acoustic emission to temporal and spatial crack motion on a microscopic scale in polymers and carbon fibres”.

References

1. C Sklarczyk, S Winkler, B Thielicke, ‚Die elektrische Emission beim Versagen von Faserverbundwerkstoffen und ihren Komponenten‘ Mat.-wiss. u. Werkstofftech. 27 559–66, 1996
2. P Koktavy, ‘Experimental study of electromagnetic emission signals generated by crack generation in composite materials’ Meas. Sci. Technol. 20 8pp, 2009
3. P Sedlak, M Enoki, T Ogasawara, J Sikula, ‚Electromagnetic and Acoustic Emission in PEEK/Carbon Nanotube Composites‘ 29th European Conference on Acoustic Emission Testing. ‚Vienna, 2010
4. I Yamada, K Masuda, H Mizutani, ‚Electromagnetic and acoustic emission associated with rock fracture‘ Phys. Earth Planet. Int. 57 157–68, 1989

5. A Misra, R C Prasad, V S Chauhan, B Srilakshmi, ‚A theoretical model for the electromagnetic radiation emission during plastic deformation and crack propagation in metallic materials‘ Int. J. Fract. 2 99–121, 2007
6. A Rabinovitch, A Shay, R Liraz, V Frid, D Bahat, ‚Electromagnetic radiation emitted during friction process‘ Int. J. Fract. 2 21–27, 2005
7. A Tsutsumi, N Shirai, ‚Electromagnetic signals associated with stickslip of quartz-free rocks‘ Tectonophysics. 1-4 79–84, 2008
8. V Frid, A Rabinovitch, D Bahat, ‚Fracture induced electromagnetic radiation‘ J. Phys. D: Appl. Phys. 36 1620-8, 2003
9. P Sedlak, J Sikula, T Lokajicek, Y Mori, ‚Acoustic and electromagnetic emission as a tool for crack localization‘ Meas. Sci. Technol. 19 7pp, 2008
10. S G O'Keefe, D V Thiel, ‚A Mechanism for the production of Electromagnetic Radiation during the fracture of Brittle Materials‘ Phys. Earth and Planet. Inter. 89 127–35, 1995
11. S Winkler, ‚Tear detector for mechanical loading test sample - uses capacitive sensor coupled via impedance converter to electronic evaluation circuit‘ patent DE 4004171 C2, 1993
12. M G R Sause, ‚In-situ monitoring of fiber-reinforced composites‘ Springer-International, Cham, 2016
13. S O Gade, U Weiss, M A Peter, M G R Sause, ‚Relation of Electromagnetic Emission and Crack Dynamics in Epoxy Resin Materials‘ J. Nondestruct. Eval. 4 711-23, 2014
14. M G R Sause, S Richler, ‚Finite Element Modelling of Cracks as Acoustic Emission Sources‘ J Nondestruct Eval 34 1-13, 2015